

MedChemComm

Accepted Manuscript



This article can be cited before page numbers have been issued, to do this please use: M. M. Nagiec, J. Duvall, A. Skepner, E. Howe, J. Bastien, E. Comer, J. Marie, S. Johnston, J. Negri, M. Eichhorn, J. Vantourout, C. Clish, K. Musunuru, M. Foley, J. Perez and M. Palmer, *Med. Chem. Commun.*, 2018, DOI: 10.1039/C8MD00297E.



This is an Accepted Manuscript, which has been through the Royal Society of Chemistry peer review process and has been accepted for publication.

Accepted Manuscripts are published online shortly after acceptance, before technical editing, formatting and proof reading. Using this free service, authors can make their results available to the community, in citable form, before we publish the edited article. We will replace this Accepted Manuscript with the edited and formatted Advance Article as soon as it is available.

You can find more information about Accepted Manuscripts in the [author guidelines](#).

Please note that technical editing may introduce minor changes to the text and/or graphics, which may alter content. The journal's standard [Terms & Conditions](#) and the ethical guidelines, outlined in our [author and reviewer resource centre](#), still apply. In no event shall the Royal Society of Chemistry be held responsible for any errors or omissions in this Accepted Manuscript or any consequences arising from the use of any information it contains.



ARTICLE

Novel Tricyclic Glycal-based *TRIB1* Inducers that Reprogram LDL Metabolism in Hepatic Cells

Received 00th January 20xx,
Accepted 00th January 20xx

DOI: 10.1039/x0xx00000x

www.rsc.org/

Marek M. Nagiec,^a Jeremy R. Duvall^a, Adam P. Skepner^a, Eleanor A. Howe^a, Jessica Bastien^a, Eamon Comer^a, Jean-Charles Marie^a, Stephen E. Johnston^a, Joseph Negri^a, Michelle Eichhorn^a, Julien Vantourout^a, Clary Clish^b, Kiran Musunuru^c, Michael Foley^a, Jose R. Perez^a, and Michelle A.J. Palmer^a

Increased expression of the Tribbles pseudokinase 1 gene (*TRIB1*) is associated with lower plasma levels of LDL cholesterol and triglycerides, higher levels of HDL cholesterol and decreased risk of coronary artery disease and myocardial infarction. We identified a class of tricyclic glycal core-based compounds that upregulate *TRIB1* expression in human HepG2 cells and phenocopy the effects of genetic *TRIB1* overexpression as they inhibit expression of triglyceride synthesis genes and ApoB secretion in cells. In addition to predicted effects related to downregulation of VLDL assembly and secretion these compounds also have unexpected effects as they upregulate expression of LDLR and stimulate LDL uptake. This activity profile is unique and favorably differs from profiles produced by statins or other lipoprotein targeting therapies. BRD8518, the initial lead compound from the tricyclic glycal class, exhibited stereochemically dependent activity and the potency far exceeding previously described benzofuran BRD0418. Gene expression profiling of cells treated with BRD8518 demonstrated the anticipated changes in lipid metabolic genes and revealed a broad stimulation of early response genes. Consistently, we found that BRD8518 activity is MEK1/2 dependent and the treatment of HepG2 cells with BRD8518 stimulates ERK1/2 phosphorylation. In agreement with down-regulation of genes controlling triglyceride synthesis and assembly of lipoprotein particles, the mass spectrometry analysis of cell extracts showed reduced rate of incorporation of stable isotope labeled glycerol into triglycerides in BRD8518 treated cells. Furthermore, we describe medicinal chemistry efforts that led to identification of BRD8518 analogs with enhanced potency and pharmacokinetic properties suitable for *in vivo* studies.

Introduction

Plasma lipoprotein and lipid profiles are heritable risk factors associated with coronary artery disease. Genome-wide association studies (GWAS) have identified ~100 loci that associate with blood lipid concentrations (1). Amongst these, a single nucleotide polymorphism (SNP) located at chromosomal locus 8q24 is significantly associated with the levels of triglycerides, low-density lipoprotein cholesterol (LDL-C) and high-density lipoprotein cholesterol (HDL-C). The minor G allele at this SNP was associated with lower triglycerides (TG), lower LDL, and higher HDL, a unique pattern for any lipid modifying SNP. The SNP is located in the 3'-downstream region of the gene encoding Tribbles pseudokinase 1 (*TRIB1*). More recent reports indicate that the minor SNP allele, which is associated with reduced risk of CAD and MI, increases the level of *TRIB1* mRNA (2). The association of *TRIB1* with CAD has been further validated by the larger GWAS study conducted by the CARDIoGRAMplusC4D Consortium (3) and replicated in populations of various ethnic backgrounds (4-6). *TRIB1* is a serine threonine kinase-like protein, which lacks a catalytic domain. The precise molecular function of *TRIB1* is unknown but it is proposed to act as

an adaptor protein in multiple pathways, including the MAPK cascade. Over-expression of *TRIB1* in the liver results in suppression of hepatic secretion of very-low-density lipoprotein (VLDL) particles, the precursor of LDL particles, improved plasma lipoprotein profile, and reduction in expression of genes encoding proteins involved in *de novo* lipogenesis (7). Beyond this, *TRIB1* has recently been implicated in macrophage differentiation and diabetes (8). Using a cell-based screen of ~9K compounds from a Diversity Oriented Synthesis (DOS) screening collection (9, 10), we identified two classes of lead compounds, benzofurans and tricyclic glycals, which induce *TRIB1* mRNA. In HepG2 cells, both classes of compounds exhibit time- and dose-dependent effects on *TRIB1* expression. In parallel, these compounds induce *LDLR* mRNA and protein, increase LDL clearance and reduce *PCSK9* mRNA expression and *PCSK9* levels in the media. The structure activity relationship for induction of *TRIB1* mirrors that for induction of *LDLR* and suppression of *PCSK9*. Whereas the benzofuran series was described previously (11), here we present a more detailed characterization of the second, more potent series of tricyclic glycals exemplified by BRD8518, which was undertaken in an effort to better define its mechanism of action. In addition we present derivatives of BRD8518 with further enhanced potency and an improved pharmacokinetic profile, which were obtained through a targeted medicinal chemistry effort.

Results and discussion

The initial lead compound BRD8518 was developed following the screen of the DOS-derived small-molecule library for compounds

^a Therapeutics Platform, Broad Institute of MIT and Harvard, Cambridge, MA02142. E-mail: marek@broadinstitute.org

^b Metabolite Profiling Platform, Broad Institute of MIT and Harvard, Cambridge, MA02142.

^c Department of Stem Cell and Regenerative Biology, Harvard University, Cambridge, MA 02138.

E-mail: marek@broadinstitute.org; Tel: +617-714-7377

ARTICLE

MedChemComm

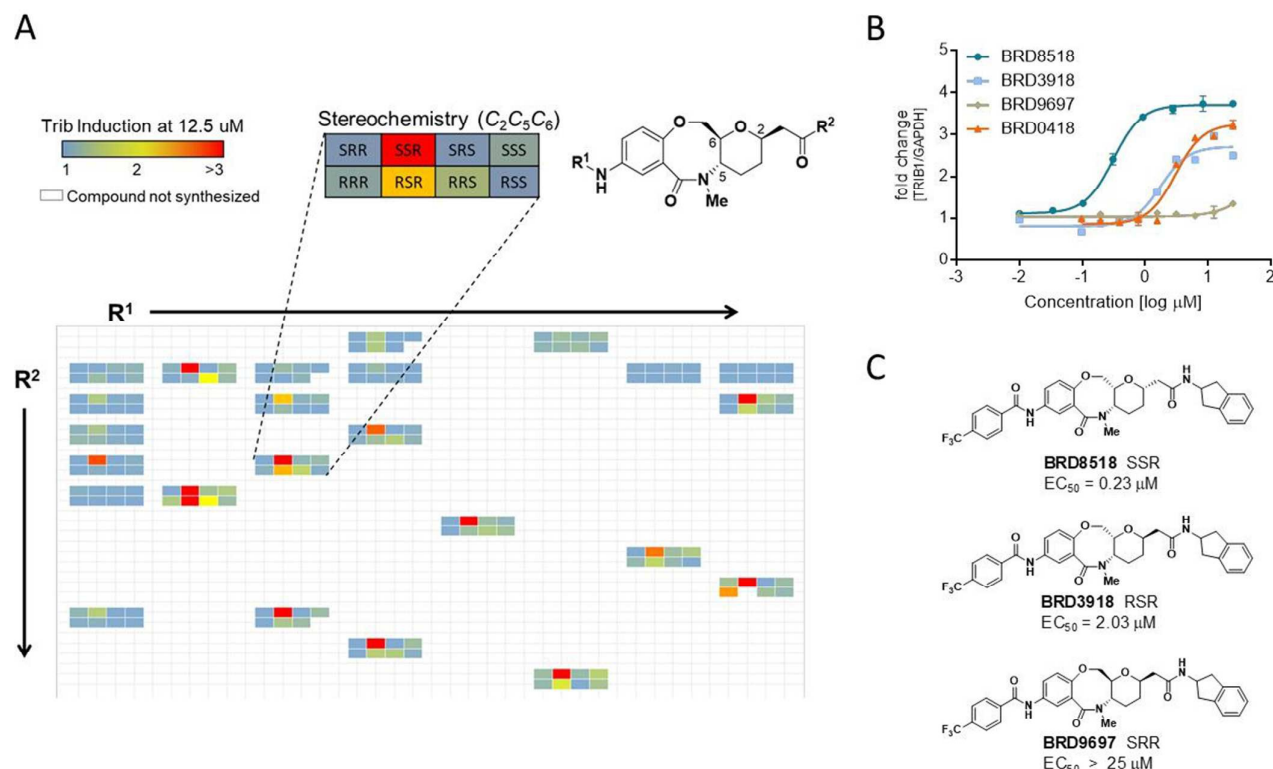


Figure 1. A qRT-PCR screen of HepG2 cells identified a series of *TRIB1* inducers from tricyclic glycal library. (A) Stereochemical dependency of the tricyclic glycal compounds revealed by the analysis of the primary screening data. Each block of eight fields represents eight stereoisomers tested in the primary screen. (B) Dose dependent up-regulation of *TRIB1* mRNA relative to GAPDH calibrator control. (C) Chemical structures of *TRIB1* inducers.

that upon 20 hour incubation at 12 μM concentration upregulated expression of *TRIB1* in HepG2 cells (Figure 1). From the confirmed hit compounds that (i) upregulated *TRIB1* expression in two hepatocellular cell lines, (ii) had no apparent cytotoxicity and (iii) inhibited the secretion of the VLDL marker ApoB from HepG2 cells, a series of tricyclic glycal-based hits (10) stood out and demonstrated stereochemically-dependent activity. BRD8518, which was not present in the initial screening collection, was synthesized by introducing the stereochemically preferred SSR configuration to the most potent hit of the series, BRD3918. This modification resulted in about 10-fold increase in potency over BRD3918 as well as the previously described lead benzofuran BRD0418 (11) (Figure 1B, C and Figure 2A). Alternatively, the SRR

configuration in BRD9697 resulted in a compound with no observed activity at the highest concentration tested. From the initial 'sparse matrix' (12) designed tricyclic glycal library (10), SAR was observed in the HTS at both R^1 and R^2 appendage sites, visualized in figure 1A (13), but the trifluoromethyl phenyl amide and indane motifs were superior at the respective positions. BRD8518 was characterized further and showed improved potency in inhibiting ApoB secretion, indicating inhibition of VLDL secretion, as predicted based on known effect of *TRIB1* overexpression on inhibition of lipogenesis

(7) (Figure 2B). Early in the hit triage process the *TRIB1* upregulating compounds were profiled in the Luminex gene expression assay to measure differential expression of 1000 selected landmark genes (L1000) (14). The L1000 data analysis

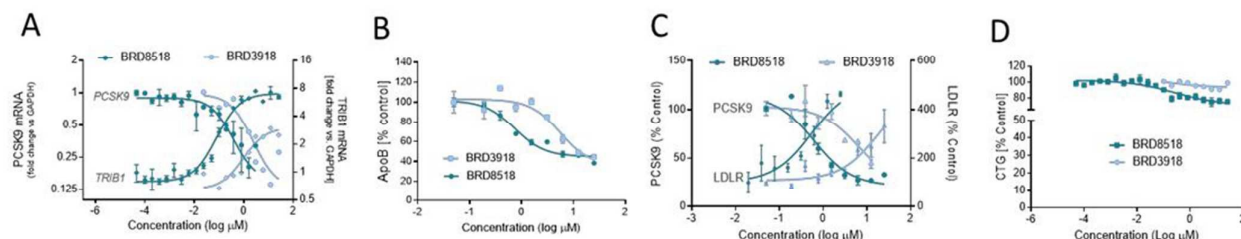


Figure 2. BRD8518 modulates expression of the key genes involved in VLDL production and in LDL clearance in HepG2 cells. Transcript levels were measured by qRT-PCR in HepG2 cells 6 hours (*TRIB1*) and 24 hours (*PCSK9*) after treatment with a dilution series of BRD3918 and BRD8518 (A). The levels of secreted ApoB and PCSK9 proteins were measured in the media by ELISA 24 hours post treatment (B, C). The level of LDL receptor protein was measured using ELISA in the cell lysates obtained 24 hours after the treatment in indicated concentrations of compounds (C). The cellular levels of ATP were not affected by BRD3918 and only slightly affected by highest concentrations of BRD8518 treatment as measured by the Cell-titer-Glo assay (D).

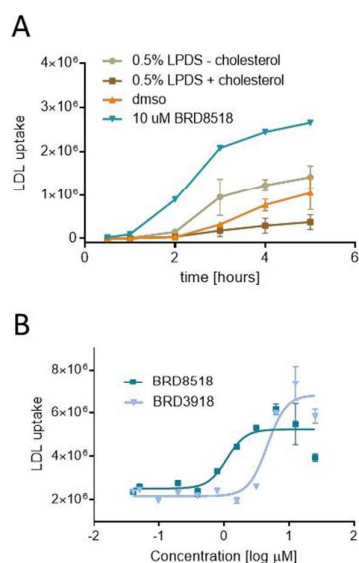


Figure 3. TRIB1 inducers stimulate uptake of LDL in HepG2 cells. (A) HepG2 cells grown under standard culture conditions (10% FBS) were treated for 20 hours with compounds BRD-3918 and BRD8518 at indicated concentrations and the uptake of BODIPY-FL conjugated LDL particles was monitored for 5 hours using high content microscopy. To control for regulation of LDL uptake by cholesterol the cells were grown in the media depleted for cholesterol (0.5% LPDS) or supplemented with cholesterol (0.5% LPDS plus cholesterol (10mg/ml cholesterol and 1mg/ml 25-OH cholesterol). (B) Dose dependent effect of BRD8518 on LDL uptake.

revealed that BRD3918 and other tricyclic glycol hits affected expression of cholesterol metabolic genes and in subsequent studies we established that BRD3918 stimulated expression of LDL receptor protein and inhibited secretion of PCSK9 protein from HepG2 cells (data not shown). Here we found that BRD8518 was also more potent than BRD3918 in downregulating secretion of PCSK9 protein (Figure 2C), upregulating expression of LDL receptor protein (Figure 2C), and, as a functional consequence, stimulating LDL uptake in HepG2 cells (Figure 3). The effects of *TRIB1* upregulating compounds in the LDL uptake pathway were unexpected and, apparently, are not driven by upregulation of *TRIB1* expression as HepG2 cells transfected with *TRIB1* expressing plasmids have unchanged levels of *PCSK9* and *LDLR* transcripts (data not shown).

Since *TRIB1* overexpression achieved by cDNA transfection was reported to inhibit the rate of triglyceride synthesis in HepG2 cells (7), we measured effects of BRD8518 on the rate of incorporation of stable isotope-labeled glycerol into triglycerides. In HepG2 cells preincubated with 2 μM BRD8518 for 24 hours, the rate of ¹³C₃-D₅-glycerol incorporation into individual triglycerides was significantly suppressed for all eight species of triglycerides that were monitored by mass spectrometry in lipid extracts (Figure 4). To begin defining the mechanism of action of BRD8518, we performed a complete gene-expression profiling experiment in HepG2 cells treated for 6 and 24 hours with 1 μM BRD8518 and we identified genes differentially expressed in response to compound treatment compared to DMSO vehicle treatment (GEO accession number: GSE57753). In addition, we profiled cells treated for 1 and 24 hours with 100 ng/ml of oncostatin M (OSM), a cytokine involved in liver

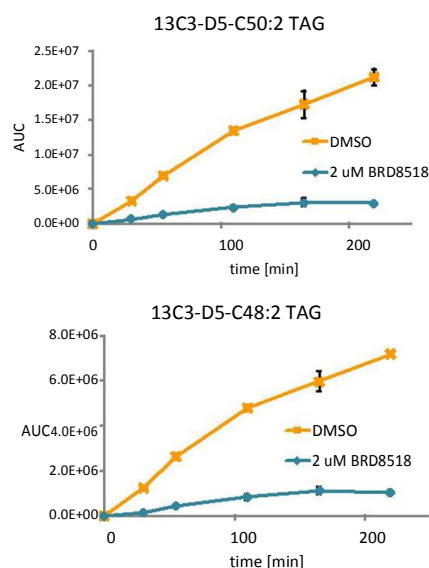


Figure 4. TRIB1 inducers attenuate the rate of triglyceride synthesis in HepG2 cells. HepG2 cells were incubated with 2 μM compound BRD8518 for 24 hours and then incubated with the stable isotope labeled glycerol (13C₃-D₅-glycerol) for varying amounts of time. The incorporation of the 13C₃-D₅-glycerol into triglycerides was quantified in the lipid extracts by high resolution mass spectroscopy. The plots show incorporation of 13C₃-D₅-glycerol into two of the species of triacylglycerol as indicated.

development. The OSM treatment was included based on our observation that OSM induced responses in HepG2 cells that resembled responses to BRD8518 including the upregulation of *TRIB1* and *LDLR* expression and the downregulation of *PCSK9* (Figure 5). The time course observed for BRD8518 induction of *TRIB1* and *LDLR* was different than that observed for OSM, which produced peak of responses at 1 hour followed by decay to

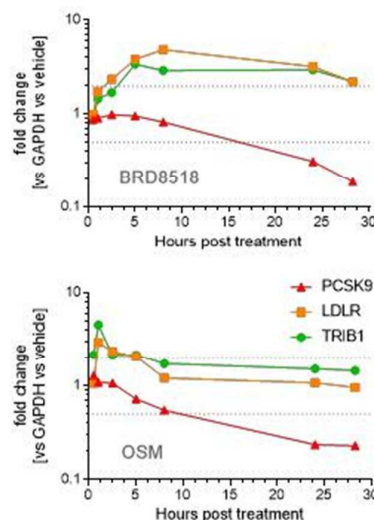


Figure 5. Kinetics of gene expression modulation over a 28 hour time course after treatment with 2.5 μM BRD8518 or 100 ng/ml oncostatin M.

ARTICLE

MedChemComm

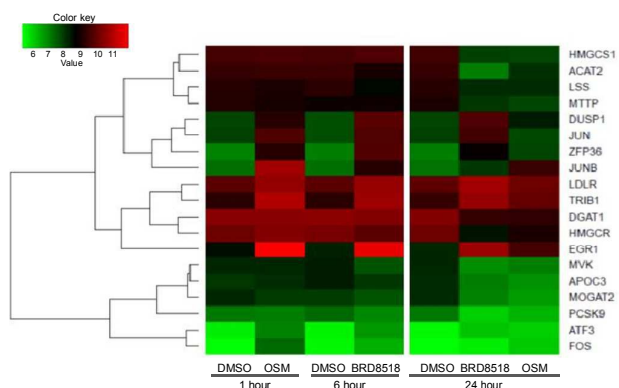


Figure 6. Genes differentially expressed in response to treatment of HepG2 cells with BRD8518 and OSM. Heat map of normalized gene expression values obtained from Affymetrix microarray hybridization experiments using RNA isolated from HepG2 cells treated with 1 μ M BRD8518 and 100 ng/ml Oncostatin M. Values below mean expression level are represented by green and values above the mean are represented by red color.

background levels within 6 hours. Maximal induction of *TRIB1* and *LDLR* was achieved at 6 hours with BRD8518 treatment and was stable up to 24 hrs later suggesting that both agents may trigger response of the same regulatory network through interaction with different triggering targets. Evaluation of Affymetrix gene expression profiling data confirmed upregulation of *TRIB1* and *LDLR* expression at earlier time points (6 hour for BRD8518 and 1 hour for OSM) and downregulation of *PCSK9* expression 24 hours post treatment. In addition, the 24 hour treatment with both BRD8518 and OSM resulted in broad downregulation of lipid metabolic genes including genes involved in triacylglycerol biosynthesis (*DGAT1*, *MOGAT2*), lipoprotein assembly (*MTP*, *APOC3*) and cholesterol biosynthesis (*HMGCS1*, *HMGCR*, *ACAT2*, *MVK*, *LSS*) (Figure 6). Early

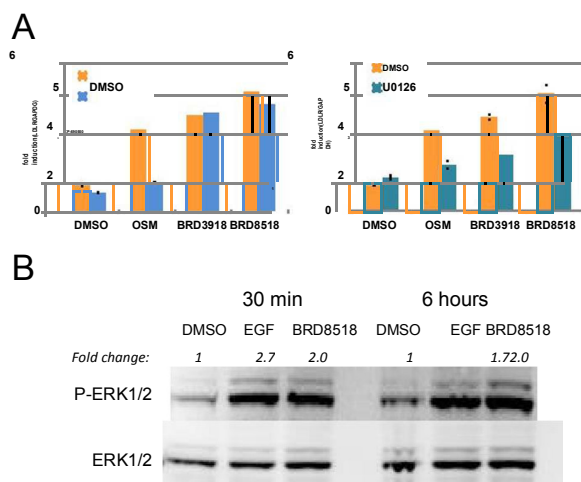


Figure 7. Induction of LDLR by BRD8518 depends on MAPK signaling. HepG2 cells were pretreated for 1 hour with 1 μ M JAK inhibitor CP-690550 (left panel) or 5 μ M MEK inhibitor U-0126 (right panel) and then treated with 100 ng/ml oncostatin M (OSM) for 1 hour and 10 μ M BRD-3918 or 2.5 μ M BRD8518 for 6 hours and examined for LDLR expression by qRT-PCR. (B) Western blot analysis of cell lysates from HepG2 cells treated for 20 hours with 100 ng/ml EGF or 2 μ M BRD8518.

response to both treatments was also broad and it included upregulation of 122 genes in response to OSM and of 180 genes in response to BRD8518. Gene set enrichment analysis pointed to significant upregulation of classic immediate early response genes such as *JUNB*, *EGR1*, *FOS*, *JUN*, *DUSP1*, *ZFP36*, *ATF3* and genes that were described to be induced as part of immediate early response in some cells like *LDLR* (15) (Figure 6). Transcript levels of *SREBF1* and *SREBF2*, transcription factors controlling expression of cholesterol pathway genes, remained unchanged by any treatment. In many respects responses to BRD8518 treatment resembled responses to OSM, a cytokine that was previously reported to stimulate LDLR expression and to reduce LDL and TG levels in hyperlipidemic animals (16). BRD8518 treatment produced expression changes in a larger number of genes, particularly at the later 24 hour time point, than OSM treatment suggesting that BRD8518 is less specific and may perturb additional pathways. Induction of early response genes suggested that upregulation of *TRIB1* and *LDLR* expression may depend on stimulation of MAP kinase signaling pathways. To test this notion we evaluated effects of two specific kinase inhibitors on ability of OSM and BRD8518 to stimulate *LDLR* expression. CP-69550 (a JAK inhibitor, which blocks receptor proximal signaling) and U01260 (a MEK inhibitor, which blocks MAPK^{Erk} signaling cascade) were used to pre-treat HepG2 cells for 1 hour prior to treatment with BRD8518 or OSM. The activity of OSM was both JAK- and MEK-dependent, whereas activity of BRD8518 was inhibited by the MEK inhibitor, but not by the JAK inhibitor (Figure 7A). Upregulation of *TRIB1* expression showed similar sensitivity to U0126 (data not shown). Subsequently we examined the ability of BRD8518 to directly stimulate ERK1/2 phosphorylation. In HepG2 cells treated with 2 μ M BRD8518, the ratio of phospho-ERK1/2 to total ERK1/2 detected by Western blot was increased 2-fold comparing to cells treated with the vehicle control as soon as 30 minutes after the treatment and remained elevated at 6 hours post treatment (Figure 7B). These results indicate that BRD8518 affects target(s) operating downstream of JAK and upstream from ERK in the MAPK signaling pathway leading to MEK1/2 dependent upregulation of *TRIB1* and *LDLR* expression. Other notable treatments that have been reported to stimulate ERK phosphorylation and LDL uptake in hepatoma cells include: HGF (17), FGF21 (18), PMA (19) and AICAR (20).

Since upregulation of LDLR stimulated by BRD8518 occurs via ERK1/2-dependent signaling and since BRD8518 downregulates other genes involved in cholesterol metabolism its mechanism of action appears to be independent of canonical SREBP2 regulation. To examine this notion further we tested the effects of BRD8518 on HepG2 cells subjected to cholesterol depletion. Incubation of HepG2 cells in cholesterol depleted media stimulated expression of *LDLR* and *PCSK9* genes, as expected due to coordinated regulation of those genes by SREBP2, and had no effect on *TRIB1* expression. BRD8518 treatment of HepG2 cells in cholesterol depleted media led to an additional upregulation of *LDLR* expression and to a significant downregulation of *PCSK9* expression indicating that the effects of BRD8518 are additive with the effects of cholesterol starvation (Figure 8A). In addition, we determined that effects of BRD8518 are additive with effects of statins, which stimulate the state of cholesterol depletion pharmacologically through inhibition of HMGCoA reductase. Stimulation of *LDLR* by treatment of HepG2 cells with simvastatin was potentiated by BRD8518 co-treatment, whereas stimulation of *PCSK9* expression by atorvastatin was

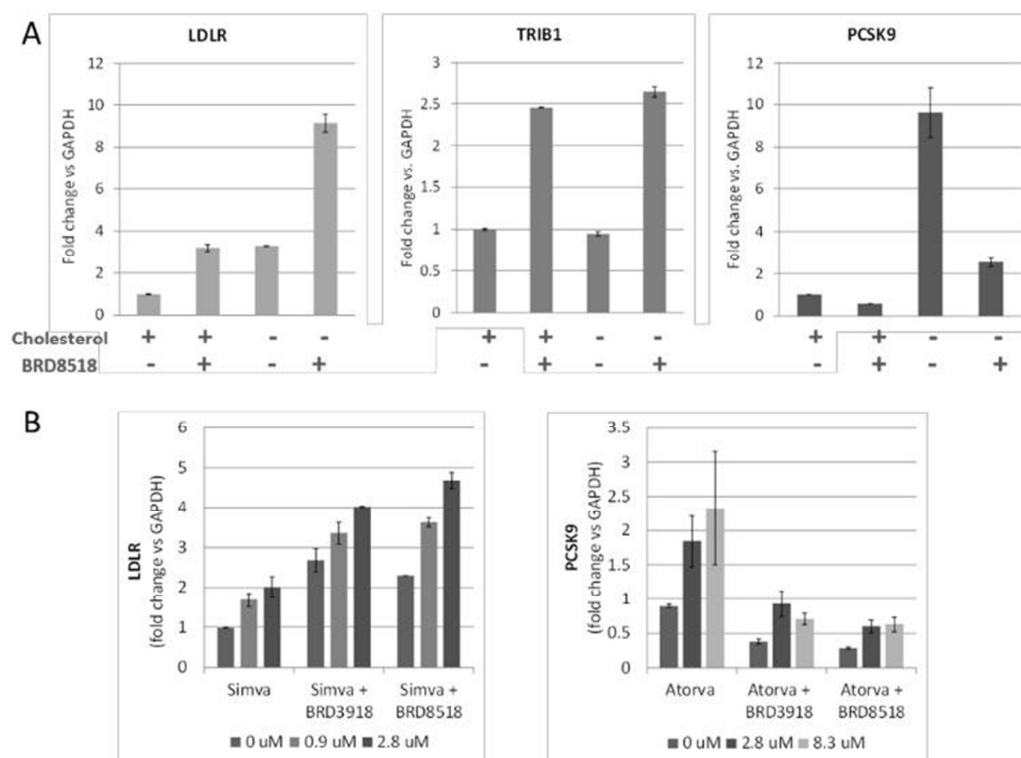


Figure 8. Effects of *TRIB1* inducers on *LDLR* and *PCSK9* expression are additive with effects of cholesterol depletion and with effects of the treatment with statins. (A) HepG2 cells pre-grown for 24 hours in the lipoprotein depleted media in the presence or absence of cholesterol were treated with 2.5 μ M BRD8518 or with DMSO and the levels of transcripts were measured by qRT-PCR 6 hours (for *LDLR*) and 24 hour (for *PCSK9*) after compound treatment.

(B) HepG2 cells pre-grown for 24 hours in the presence of indicated concentrations of statin were treated for 6 hours (left panel) or for 24 hours (right panel) with 10 μ M BRD3918, 2 μ M BRD8518 and the levels of *LDLR* (left panel) and *PCSK9* (right panel) transcripts were quantified by qRT-PCR.

opposed by co-treatment with BRD8518 (Figure 8B).

The potency and ADME profile of BRD8518 indicated it was not suitable for *in vivo* testing and medicinal chemistry work was undertaken to improve its potency and physical chemical properties with the goal of identifying a compound for *in vivo* proof of concept

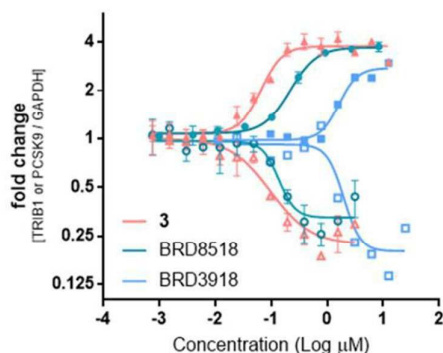


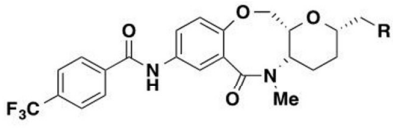
Figure 9. Improved potency of cpd **3** in transcript modulation assays in comparison to the screening hit BRD3918 and the initial lead BRD8518. Transcript levels were measured by qRT-PCR in HepG2 cells treated for 6 hours for *TRIB1* (solid symbols) and for 24 hours for *PCSK9* (open symbols) with a dilution series of indicated compounds.

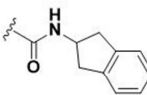
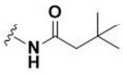
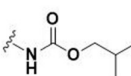
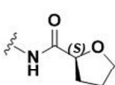
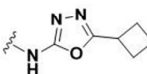
studies. The liver cell biomarkers *TRIB1*, *LDLR* and *PCSK9*, were used to drive chemistry optimization of potency. Changes to solubility, mouse and human microsomal stability, plasma stability, plasma protein binding and ATP levels in HepG2 cells were also monitored. Efforts were primarily focused on the two appendage sites, R^1 and R^2 . Modification at R^1 generally resulted in a loss of activity, including relatively minor changes such as positional changes of the CF_3 moiety on the aromatic ring. Changes at R^2 were better tolerated and hit to lead optimization produced a number of promising molecules with improved stability and increased potency against the liver cell biomarkers (Figure 9, Table 1). The best molecules (**3** and **5**), as assessed by maintaining or improving potency while also improving solubility and stability, were chosen for *in vivo* pharmacokinetic assessment. Plasma PK parameters for **1** (BRD8518), **3** and **5** are listed in Table 2. At a single dose of 10mg/kg delivered by IP injection **3** gave the best liver exposure based on calculation of free fraction (f_u values for **1**, **3** and **5** were 0.01, 0.01 and 0.02, respectively) and the potency measured in HepG2 cells. *In vivo* dial-up PK with **3** was carried out at four concentrations at single dose (10, 15, 30 and 45 mg/kg, IP). At the 15, 30 and 45 mg/kg dose, acceptable level of the required concentration of **3** was observed at 8–12 hrs post dose, indicating that BID dosing would be required for full target coverage. At all doses including the highest dose of 45 mg/kg, no adverse effects were observed over 24 hrs.

The molecular target of BRD8518 is currently unknown, however our data indicate that its perturbation produces a broad response

ARTICLE

MedChemComm

Table 1. Activity of R2 substituted tricyclic glycals in RT-qPCR assays for *TRIB1*, *LDLR* and *PCSK9* modulation in Hap1 cells and in *in vitro* pharmacokinetics assessment of solubility and mouse liver microsomal stability.


Compound	R	<i>TRIB1</i> upregulation ^a EC ₅₀ (μM) [max induction]	<i>LDLR</i> upregulation ^a EC ₅₀ (μM) [max induction]	<i>PCSK9</i> downregulation ^b EC ₅₀ (μM) [% inhibition]	Solubility ^c [μM]	Microsomal stability ^d
1 (BRD8518)		0.43 [4.7]	0.49 [4.8]	0.24 [76.5]	0	0
2		0.72 [6.6]	0.5 [1.9]	0.1 [80]	6	0
3		0.08 [5.8]	0.17 [3.7]	0.06 [77]	7	28
4		1.1 [3.7]	2.45 [4.3]	0.025 [85]	90	54
5		0.32 [4.6]	1.45 [3.8]	0.095 [81.5]	27.5	18

^a 6 hour treatment. ^b 24 h treatment. ^c in 1% DMSO in PBS. ^d % remaining after 1 hour incubation. EC₅₀ values represent average of two or more replicates.

that involves activation of MAPK^{erk} signaling followed by upregulation of number of early response genes including *TRIB1* and *LDLR* and leads to remarkable changes in the lipoprotein metabolism, resulting in a decrease in VLDL production and an upregulation of LDL uptake in cells of hepatic origin. The profile of hepatic cells responses evoked by BRD8518 and its analogues is similar to previously described responses to known hypolipidemic agents, a natural product berberine and the endogenous cytokine oncostatin M (OSM). Cpd **3** is the most potent molecule in the class of *TRIB1* inducers and its discovery will enable *in vivo* proof of concept studies and will enhance target identification efforts and uncovering of the molecular nature of this novel hepatic regulatory mechanism with potential therapeutic utility.

Experimental

Materials and methods

Cell culture and chemicals. Growth media for HepG2 cells (ATCC) contained DMEM High glucose with sodium pyruvate and glutamine (Invitrogen), 10% FBS (Hyclone), Penicillin (100 units/mL), Streptomycin (100 μg/mL) and glutamine (2 mM) (Invitrogen). HepG2 cells were cultured at 37°C, 5% CO₂. For

cholesterol depletion experiments cells were grown in the DMEM media containing the indicated concentration of the lipoprotein deficient serum (LPDS, Sigma). Oncostatin M was obtained from R&D Systems. Berberine (Sigma) and the compounds from the screening collection were prepared as 10 mM solutions in DMSO, diluted appropriately in DMSO and delivered to cell culture at indicated concentrations keeping the concentration of vehicle constant at 0.25%.

Compound screening and generation of cDNA. HepG2 cells were plated in 40 μL of growth media in white 384 well plates

Table 2. Pharmacokinetic parameters of **1** (BRD8518), **3** and **5** in plasma and liver following a single intraperitoneal administration in male C57BL/6 mice at 10 mg/kg dose.

	1 (BRD8518)		3		5	
	Plasma	Liver	Plasma	Liver	Plasma	Liver
T _{max} (hr)	1.00	0.08	0.50	0.08	1.00	1.00
C _{max} (μg/L)	437	4658	2307	13127	3047	13824
AUC _{inf} (μg/L*hr)	1010	11558	3616	16803	6464	35928
T _{1/2} (hr)	1.63	2.25	1.12	1.16	1.46	1.78
Cl (L/hr/kg)	9.89	0.87	2.77	0.60	1.55	0.28
V _z (L/kg)	23.30	2.81	4.48	0.99	3.26	0.72

(Corning) and incubated overnight. The next day 100 nanoliters of compound was transferred to the plates using CyBio Well pinning tool and incubated overnight. After 18–22 hr of incubation RNA was harvested and cDNA was synthesized using the Ambion Cells-to-CT reagents (Life Technologies). Specifically, the cells were washed 2x with PBS and then lysed with 10 μ L of Cells-to-CT Lysis with DNase reagent and incubated at room temperature for 10 minutes. After the incubation 1 μ L of Stop solution was added. Two μ L of the RNA lysis was added to 8 μ L of Cells-to-CT cDNA reagent in a 384 well plate (Axygen) and incubated as follows: 37 °C for 1 hr, 95 °C for 5 min then 4 °C until frozen at -80 °C.

Gene expression analysis by qRT-PCR. Gene expression was measured by quantitative PCR in a 5 μ L reaction in a 384 well plate (Roche) as follows: 2.5 μ L Probes Master Mix (Roche)

Table 3. RT-qPCR primer / probes.

Gene	Assay ID/Sequence	Source
TRIB1	Hs00921832_m1	Applied Biosystems
GAPDH	4326317E	Applied Biosystems
B2M	4310886E	Applied Biosystems
PCSK9	Hs.PT.49a.3004786	IDT
LDLR	Hs.PT.49a.20193252	IDT

0.125 μ L of human target gene primer/probe, 0.125 μ L of human calibrator gene primer/probe (GAPDH or B2M) and 1.25 μ L of PCR grade water. The identities and sources of the primer/probe sets used are listed in Table 3. Thermocycling was performed in a Roche Light Cycler 480 II instrument using

the following conditions: 95°C for 10 minutes, 95°C for 10s, 60°C for 30s for 55 cycles then 40°C for 30s. Relative gene expression was calculated using the equation 2^{-CT} (21).

Transcriptional profiling. (GEO accession number: GSE57753) HepG2 cells were plated in a black 96-well tissue culture plate (Corning 3904) in 100 μ L of DMEM/10% FBS/1x Pen-Strep-Glutamine media at the density of 10,000 cells per well. The cells were incubated overnight in a tissue culture incubator at 37°C and 5% CO₂. The cells (6-wells each treatment) were treated with 1 μ M BRD8518 for 6 hr at 37°C. The cells were also treated with ML8518 (1 μ M) or Oncostatin M (100 ng/mL) for 1 hr and 24 hr at 37°C. DMSO controls were set up for each time point. Compounds were added to the cells to a final DMSO concentration of 0.25%. Oncostatin M was dissolved in PBS and DMSO was added to the wells to bring the final concentration to 0.25%. RNA was prepared using RNeasy Minipreps (Qiagen) following the manufacture's protocol. Biotin labeling was performed using the Ambion WT Expression Kit (Life Technologies, Grand Island, NY) according to the manufacturer's protocol, followed by the GeneChip WT Terminal Labeling and Controls Kit (Affymetrix, Santa Clara, CA). The labeled, fragmented DNA was hybridized to the Affymetrix GeneChip Human Gene ST 2.0 Array for 18 hours in a GeneChip Hybridization oven 640 at 45°C with rotation (60 rpm). The hybridized samples were washed and stained using Affymetrix fluidics station 450 with streptavidin-R-phycoerythrin (SAPE) and the signal was amplified using a biotinylated goat anti-streptavidin antibody followed by another SAPE staining

(Hybridization, Washing and Staining Kit, Affymetrix, Santa Clara, CA). The hybridized samples were washed and stained using an Affymetrix fluidics station 450. After staining, microarrays were immediately scanned using an Affymetrix GeneArray Scanner 3000 7G Plus. All procedures were performed at Boston University Microarray Resource Facility exactly as described in Affymetrix GeneChip Expression Analysis Technical Manual (Affymetrix, Santa Clara, CA, current version available at www.affymetrix.com). Data were normalized using the Robust Multi-Array Average method as implemented in the R package oligo (22). Differential expression analysis was performed using the R package limma (23).

ELISA assays. HepG2 cells were plated in black clear bottom (Costar) 96-well plates at 40,000 cells/well in 100 μ L of growth media. On Day 2 media was changed and cells were treated with compounds for 24 hr. After 24 hr medium was removed and used for the PCSK9 (R&D Systems) and apoB (Mab Tech) ELISAs. For the apoB and PCSK9 ELISAs 50 μ L and 10 μ L of medium were used, respectively. For the LDLR ELISA (R&D Systems), cells were washed once with PBS (Invitrogen), lysed with 100 μ L PBS/0.1% Igepal (Sigma) and frozen at -80 °C until analyzed. Ten μ L of lysate was used for the analysis.

Cell viability assay. HepG2 cells were plated in white 384 well plates (Corning) at 2000 cells/well in 40 μ L of growth medium and incubated overnight at 37°C with 5% CO₂. The next day cells were treated with 100 nL of compound for 24 hr. Cellular ATP levels were measured using CellTiter-Glo (Promega).

Stable isotope labeling and analysis of triglycerides in HepG2 cells. The cells were plated at 40,000 cells/well in 96-well plate in growth media, incubated overnight and then treated for 24 hours with compounds as indicated. For stable isotope labeling of TG the cells were washed with PBS, incubated for at least 15 minutes with DMEM supplemented with 25 mM HEPES (pH 7.5) containing 0.1% FAF-BSA and then after media replacement incubated at 37°C with DMEM containing 25 mM HEPES (pH7.5), 0.1 % FAF-BSA and 20 μ M ¹³C₃-D₅-glycerol for indicated periods of time. The lipids were extracted after the media removal by incubating the cells with 150 μ L isopropanol at room temperature for 15 min with shaking. The cell extracts (120 μ L) were cleared by centrifugation and concentrated 5-fold through drying and resuspension in isopropanol. Liquid chromatography-tandem mass spectrometry (LC-MS) analyses of cell extracts were conducted using an Open Accela 1250 U-HPLC coupled to a Q Exactive hybrid quadrupole orbitrap mass spectrometer (Thermo Fisher Scientific; Waltham, MA). Extracts (10 μ L) were injected directly onto a 150 x 3.0 mm Prosphere HP C4 column (Grace, Columbia, MD). The column was eluted isocratically at a flow rate of 350 μ L/min with 80% mobile phase

A (95:5:0.1 vol/vol/vol 10 mM ammonium acetate/methanol/acetic acid) for 2 minutes followed by a linear gradient to 80% mobile phase B (99.9:0.1 vol/vol methanol/acetic acid) over 1 minute, a linear gradient to 100% mobile phase B over 12 minutes, and then 10 minutes at 100% mobile-phase B. MS analyses were conducted using electrospray ionization in the positive ion mode using full scan analysis at 70,000 resolution and 3 Hz data acquisition rate.

ARTICLE

MedChemComm

Monoisotopic and ^{13}C -D5-TAG LC-MS peaks were integrated using TraceFinder 2.0 (Thermo Fisher Scientific; Waltham, MA). **LDL uptake.** HepG2 cells were plated at 3000 cells/well in a 384 well plate (Corning) in growth medium. After an overnight incubation 10 μL of 5x compound was added and the plates were incubated overnight. The cells were then washed with phenol red free DMEM (Invitrogen) and incubated with 30 μL of BODIPY-FL-LDL (Invitrogen) diluted to final concentration 5 μg protein/ml in phenol red free DMEM for 0.1 to 5 hr. LDL uptake was stopped by fixing the cells with 3% formaldehyde. Nuclei were stained with Hoechst 33342 diluted in PBS for 10 minutes. The cells were then washed with PBS and imaged using an IXM microscope. Image analysis and quantification was performed with MetaXpress software (ver. 3.1.0.97, Molecular Devices) using the Multi Wavelength Cell Scoring application module.

Western blot analysis. HepG2 cells were seeded in 6-well plates at approximately 800,000 cells /well, incubated in growth media at 37°C for 24 hours, further incubated for 20 hours in serum-free DMEM and then treated with EGF (100 ng/ml), BRD3918 (10 μM) or BRD8518 (2 μM) for the indicated times. At the end of treatment, cells were washed with PBS and lysed in RIPA lysis buffer (50mM Tris-HCl, 1% IGEPAL, 0.5% Na-deoxycholate, 0.1% SDS, 150 mM NaCl, 2 mM EDTA, 50 mM NaF) with protease inhibitor cocktail (Roche). Lysates were incubated on ice for 1 hour with frequent agitation, centrifuged at 13,000 rpm for 15 minutes at 4°C and then equal amount of protein from each lysate (~ 50 μg) was denatured, subjected to electrophoresis using NuPAGE® Novex® 4-12% Bis-Tris Gels and transferred to PVDF membranes with iBlot Gel Transfer Device (Invitrogen) according to manufacturer's instructions. The ERK1/2 phosphorylation was detected using rabbit polyclonal antibodies directed against p44/42 MAPK (Erk1/2) and Phospho-p44/42 MAPK (Erk1/2) (Cell Signaling Technology) and the goat anti-rabbit IgG (H+L) secondary antibodies conjugated with HRP (Thermo Scientific). After standard incubations and washing the membranes were exposed with SuperSignal West Femto Maximum Sensitivity Substrate (Thermo Scientific), images captured using Kodak Image Station 4000mm PRO and Carestream Molecular Imaging Software. Band intensities were calculated using Image J software. The main text of the article should appear here with headings as appropriate. **Pharmacokinetic studies.** Plasma pharmacokinetics and liver distribution of selected compounds were performed at Sai Life Sciences (Hinjewadi, India) following animal welfare guidelines provided by the Committee for the Purpose of Control and Supervision of Experiments on Animals (CPCSEA). All study protocols were approved by both Broad Institute and Sai IACUCs. Compound concentrations were measured by mass spectrometry in plasma and liver homogenates of male C57BL/6 mice following a single intraperitoneal dose administration. The samples were collected and analysed 0.08, 0.5, 1, 2, 4 and 8 hr post injection. Pharmacokinetic parameters were assessed using the Non-Compartmental Analysis module in Phoenix WinNonlin (Version 6.3).

Solubility. Solubility was determined in phosphate buffered saline (PBS) pH 7.4 with 1% DMSO. Each compound was prepared in triplicate at 100 μM in both 100% DMSO and PBS

with 1% DMSO. Compounds were allowed to equilibrate at room temperature with a 750 rpm vortex shake for 18 hours. After equilibration, samples were analyzed by UPLC-MS (Waters, Milford, MA) with compounds detected by SIR detection on a single quadrupole mass spectrometer. The DMSO samples were used to create a two-point calibration curve to which the response in PBS was fit.

Plasma Protein Binding. Plasma protein binding was determined by equilibrium dialysis using the Rapid Equilibrium Dialysis (RED) device (Pierce Biotechnology, Rockford, IL) for both human and mouse plasma. Each compound was prepared in duplicate at 5 μM in plasma (0.95% acetonitrile, 0.05% DMSO) and added to one side of the membrane (200 μL) with PBS pH 7.4 added to the other side (350 μL). Compounds were incubated at 37°C for 5 hours with a 350-rpm orbital shake. After incubation, samples were analyzed by UPLC-MS (Waters, Milford, MA) with compounds detected by SIR detection on a single quadrupole mass spectrometer.

Microsomal Stability. Microsomal stability was determined at 37°C at 60 minutes in both human and mouse microsomes. Each compound was prepared in duplicate at 1 μM with 0.3 mg/mL microsomes in PBS pH 7.4 (1% DMSO). Compounds were incubated at 37°C for 60 minutes with a 350-rpm orbital shake with time points taken at 0 minutes and 60 minutes. Samples were analyzed by UPLC-MS (Waters, Milford, MA) with compounds detected by SIR detection on a single quadrupole mass spectrometer.

Synthetic procedures

Synthesis of BRD8518: Step1 - Methyl 2-((2S,4aS,12aR)-5-methyl-6-oxo-8-(4-(trifluoromethyl)benzamido)-2,3,4,4a,5,6,12,12a-octahydrobenzo[b]pyrano[3,2-f][1,5]oxazocin-2-yl)acetate: At 0 °C, 4-trifluoromethylbenzoyl chloride (0.49 mL, 3.3 mmol, 1.1 equiv) was added dropwise to

a solution of methyl 2-((2S,4aS,12aR)-8-amino-5-methyl-6-oxo-2,3,4,4a,5,6,12,12a-octahydrobenzo[b]pyrano[3,2-f][1,5]oxazocin-2-yl)acetate (1.0 g, 3.0 mmol, 1.0 equiv) and triethylamine (0.63 mL, 4.49 mmol, 1.5 equiv) in CH_2Cl_2 (60 mL). After complete conversion of the starting material (LCMS, 30 min), the reaction was quenched with a saturated solution of ammonium chloride (30 mL) and the crude mixture was partially concentrated. The aqueous phase was extracted with EtOAc (3x50 mL) and the combined organic phases were washed with brine, dried over Na_2SO_4 , filtered and concentrated under reduced pressure. The crude residue was purified by silica gel chromatography (gradient: 0–80% EtOAc in Hexanes), which yielded 1.2 g (2.36 mmol, 79 % yield) of methyl 2-((2S,4aS,12aR)-5-methyl-6-oxo-8-(4-(trifluoromethyl)benzamido)-2,3,4,4a,5,6,12,12a-

octahydrobenzo[b]pyrano[3,2-f][1,5]oxazocin-2-yl)acetate, as a white solid. ^1H NMR (300 MHz, CDCl_3) δ 8.66 (s, 1H), 7.98 (d, J = 8.1 Hz, 2H), 7.87 (d, J = 9.3 Hz, 1H), 7.73 (d, J = 8.1 Hz, 2H), 7.45 (d, J = 2.7 Hz, 1H), 6.82 (d, J = 9.0 Hz, 1H), 4.07 (dd, J = 12.2, 3.2 Hz, 1H), 4.02 – 3.76 (m, 4H), 3.72 (s, 3H), 3.26 (s, 3H), 2.61 (dd, J = 15.7, 7.3 Hz, 1H), 2.48 (dd, J = 15.7, 5.3 Hz, 1H), 2.21 – 2.08 (m, 2H), 1.98 – 1.80 (m, 1H), 1.80 – 1.69 (m, 1H). LRMS (ESI) calcd for $\text{C}_{25}\text{H}_{26}\text{F}_3\text{N}_2\text{O}_6$ [M + H] $^+$ 507.17, found 507.22.

Step 2 - 2-((2S,4aS,12aR)-5-methyl-6-oxo-8-(4-(trifluoromethyl)benzamido)-2,3,4,4a,5,6,12,12a-octahydrobenzo[b]pyrano[3,2-f][1,5]oxazocin-2-yl)acetic acid:

A THF solution (43 mL) of methyl 2-((2S,4aS,12aR)-5-methyl-6-oxo-8-(4-(trifluoromethyl)benzamido)-2,3,4,4a,5,6,12,12a-octahydrobenzo[b]pyrano[3,2-f][1,5]oxazocin-2-yl)acetate (1.1

g, 2.2 mmol, 1.0 equiv) was cooled in an iced bath (0 °C) and hydrogen peroxide (30 % by weight, 2.7 mL, 26.0 mmol, 12.0 equiv) was added to the mixture, followed by lithium hydroxide (1.0 M in water, 13.0 mL, 13.0 mmol, 6.0 equiv). The reaction was stirred overnight, reaching rt progressively upon which LCMS analysis showed complete disappearance of the starting

material. At 0 °C, the reaction mixture was acidified with 1N HCl solution until pH ~3, diluted with brine (75 mL) and extracted with EtOAc (3x40 mL). Combined organic layers were dried over Na₂SO₄, filtered and concentrated in vacuo to give 2-((2S,4aS,12aR)-5-methyl-6-oxo-8-(4-(trifluoromethyl)benzamido)-2,3,4,4a,5,6,12,12a-octahydrobenzo[b]pyrano[3,2-f][1,5]oxazocin-2-yl)acetic acid

as a white solid (1.1 g, 2.2 mmol), which was used in the next step without further purification. ¹H NMR (300 MHz, CDCl₃) δ 9.21 (s, 1H), 7.99 (d, J = 8.1 Hz, 2H), 7.91 (d, J = 9.8 Hz, 1H), 7.69 (d, J = 8.1 Hz, 2H), 7.47 (d, J = 2.7 Hz, 1H), 6.77 (d, J = 9.0 Hz, 1H), 4.10 – 3.88 (m, 2H), 3.87 – 3.70 (m, 3H), 3.23 (s, 3H), 2.63 (dd, J = 15.9, 7.2 Hz, 1H), 2.52 (dd, J = 15.9, 5.2 Hz, 1H), 2.19 – 2.06 (m, 2H), 1.97 – 1.82 (m, 1H), 1.82 – 1.69 (m, 1H). LRMS (ESI) calcd for C₂₄H₂₄F₃N₂O₆ [M + H]⁺ 493.16, found 493.42.

Step 3 - N-((2S,4aS,12aR)-2-(2-((2,3-dihydro-1H-inden-2-yl)amino)-2-oxoethyl)-5-methyl-6-oxo-2,3,4,4a,5,6,12,12a-octahydrobenzo[b]pyrano[3,2-f][1,5]oxazocin-8-yl)-4-(trifluoromethyl)benzamide (BRD8518):

At 0 °C, 2-aminoindane (13.7 uL, 0.1 mmol, 1.3 equiv) was added to a solution of crude 2-((2S,4aS,12aR)-5-methyl-6-oxo-8-(4-(trifluoromethyl)benzamido)-2,3,4,4a,5,6,12,12a-octahydrobenzo[b]pyrano[3,2-f][1,5]oxazocin-2-yl)acetic acid (40 mg, 0.08 mmol, 1.0 equiv) and DIEA (42.6 uL, 0.24 mmol, 3.0 equiv) in CH₂Cl₂ (0.16 mL), followed by PyBOP (67.6 mg, 0.13 mmol, 1.6 equiv). The reaction mixture was stirred overnight, reaching rt progressively. The reaction mixture was diluted with CH₂Cl₂ (10 mL) and washed with a saturated solution of ammonium chloride (2x10 mL). The aqueous phase was extracted with CH₂Cl₂ (3x10 mL) and the combined organic layers were dried over Na₂SO₄, filtered and concentrated to yield a crude material which was purified by chromatography on silica gel (gradient: 10–100% EtOAc in Hexanes). N-((2S,4aS,12aR)-2-(2-((2,3-dihydro-1H-inden-2-yl)amino)-2-oxoethyl)-5-methyl-6-oxo-2,3,4,4a,5,6,12,12a-octahydrobenzo[b]pyrano[3,2-f][1,5]oxazocin-8-yl)-4-(trifluoromethyl)benzamide (BRD8518) was isolated as an off-white solid (42 mg, 0.07 mmol, 85 % yield over two steps). ¹H NMR (300 MHz, CDCl₃) δ 8.77 (s, 1H), 7.96 (d, J = 8.1 Hz, 2H), 7.89 (dd, J = 9.1, 2.7 Hz, 1H), 7.68 (d, J = 8.2 Hz, 2H), 7.42 (d, J =

2.8 Hz, 1H), 7.30 – 7.17 (m, 4H), 6.82 (d, J = 9.0 Hz, 1H), 6.17 (d, J = 7.9 Hz, 1H), 4.81 – 4.69 (m, 1H), 3.94 – 3.81 (m, 1H), 3.79 – 3.66 (m, 4H), 3.36 (dd, J = 7.0, 4.3 Hz, 1H), 3.31 (dd, J = 6.7, 4.2

Hz, 1H), 3.16 (s, 3H), 2.83 (dd, J = 4.1, 4.1 Hz, 1H), 2.78 (dd, J = 4.0, 4.0 Hz, 1H), 2.33 (d, J = 5.9 Hz, 2H), 2.13 – 2.06 (m, 2H), 1.88 – 1.76 (m, 1H), 1.76 – 1.65 (m, 1H). LRMS (ESI) calcd for C₃₃H₃₃F₃N₃O₅ [M + H]⁺ 608.24, found 608.28.

General Synthetic details for “Reverse amide” capping on the right-side:

General protocol for Curtius reaction: At rt and under argon atmosphere, DPPA (2.0 equiv) was added dropwise to a solution of 2-((2S,4aS,12aR)-5-methyl-6-oxo-8-(4-(trifluoromethyl)benzamido)-2,3,4,4a,5,6,12,12a-octahydrobenzo[b]pyrano[3,2-f][1,5]oxazocin-2-yl)acetic acid (1.0 equiv) and triethylamine (3.0 equiv) in dry acetonitrile (0.01 M). The reaction mixture was heated at 50 °C for two hours, cooled to rt for 15 min and transferred dropwise via Pasteur pipet to an aqueous solution of 1M NaOH, under vigorous stirring and cooled at 0 °C. After 30 min, Boc₂O (10 equiv) was quickly added to the solution and the reaction mixture was stirred overnight, gradually warming to rt. Solvents were partially removed in vacuo and the mixture was extracted with CH₂Cl₂. Combined organic phases were washed with brine, dried over MgSO₄, filtered and concentrated and the residue was purified by silica gel chromatography.

General protocol for Boc deprotection: At 0 °C, trifluoroacetic acid (TFA, 20.0 equiv) was added dropwise to a solution of the appropriate Boc protected amine (1.0 equiv) in CH₂Cl₂ (0.05 M). After 10 min, the reaction mixture was warmed to rt and stirred until complete disappearance of the starting material (LCMS). The crude was then concentrated to dryness, redissolved in EtOAc and washed with a saturated solution of sodium bicarbonate until pH ~ 7. The combined aqueous phases were extracted with EtOAc and the combined organic layers were washed with brine, dried over Na₂SO₄, filtered and concentrated to give the desired product, which was used without further purification.

General protocol for amine capping:

Formation of carbamate: At 0 °C, the appropriate chloroformate (1.1 equiv) was added to a solution of the appropriate amine (1.0 equiv) and triethylamine (5.0 equiv) in CH₂Cl₂ (0.05 M). After 15 min, the iced bath was removed and the reaction mixture was stirred at rt overnight. Silica gel was then added and the crude was concentrated to dryness. Purification was done via silica gel chromatography affording the desired product.

Alternative protocol for the formation of carbamate: At 0 °C, the appropriate chloroformate (1.1 equiv) was added to a solution of the appropriate amine (1.0 equiv) in a mixture of 1,4-dioxane and saturated aqueous sodium bicarbonate solution (dioxane:sat. NaHCO₃=2:1, 0.05M concentration). Upon completion of the reaction (LCMS), extraction of the mixture with EtOAc followed by evaporation of the solvents afforded a crude residue which was purified via silica gel chromatography.

ARTICLE

MedChemComm

Formation of amide: At 0 °C, the appropriate carboxylic acid (2.0 equiv) was added to a solution of the amine (1.0 equiv) and TEA (6.0 equiv) in CH₂Cl₂/DMF (40:1 ratio, 0.05 M), followed by PyBOP (2.2 equiv). The reaction mixture was stirred overnight, reaching rt progressively. The reaction mixture was diluted with CH₂Cl₂ and washed with a saturated solution of sodium bicarbonate. The aqueous phase was extracted with CH₂Cl₂ and the combined organic layers were dried over Na₂SO₄, filtered and concentrated to yield a crude material which was purified by chromatography on silica gel.

Formation of amino oxadiazole: The appropriate oxadiazolone (1.3 equiv) was added to the appropriate amine (1.0 equiv) in DMF (0.05M), followed by DIPEA (4 equiv) and BOP (1.5 equiv). The reaction was stirred at room temperature until complete conversion was observed. The mixture was partially concentrated, taken up in EtOAc and washed with a saturated solution of sodium bicarbonate. The layers separated and the aqueous layer extracted with EtOAc. The combined organic extracts were washed with brine, dried over MgSO₄, filtered and concentrated to yield a crude material which was purified by chromatography on silica gel.

Synthesis and characterization of 3:

Isobutyl (((2S,4aS,12aR)-5-methyl-6-oxo-8-(4-(trifluoromethyl)benzamido)-2,3,4,4a,5,6,12,12a-octahydrobenzo[b]pyrano[3,2-f][1,5]oxazocin-2-yl)methyl)carbamate:

At 0 °C, trifluoroacetic acid (TFA, 0.60 mL, 7.81 mmol, 20.0 equiv) was added dropwise to a solution of

tert-butyl (((2S,4aS,12aR)-5-methyl-6-oxo-8-(4-(trifluoromethyl)benzamido)-2,3,4,4a,5,6,12,12a-octahydrobenzo[b]pyrano[3,2-f][1,5]oxazocin-2-yl)methyl)carbamate (220 mg, 0.39 mmol, 1.0 equiv) in CH₂Cl₂ (8 mL). After 10 min, the reaction mixture was warmed to rt and stirred until complete disappearance of the starting material (LCMS, 1h40min). The crude was then concentrated to dryness, redissolved in EtOAc (20 mL) and washed with a saturated solution of sodium bicarbonate until pH ~ 7. The combined aqueous phases were extracted with EtOAc (3x50 mL) and the combined organic layers were washed with brine, dried over Na₂SO₄, filtered and concentrated to give N-((2S,4aS,12aR)-2-(aminomethyl)-5-methyl-6-oxo-2,3,4,4a,5,6,12,12a-octahydrobenzo[b]pyrano[3,2-f][1,5]oxazocin-8-yl)-4-(trifluoromethyl)benzamide as a white solid (166 mg, 0.36 mmol, 92% yield) which was used without further purification. At 0 °C, isobutylchloroformate (9.3 uL, 71 umol, 1.1 equiv) was added to a solution of crude N-((2S,4aS,12aR)-2-(aminomethyl)-5-methyl-6-oxo-2,3,4,4a,5,6,12,12a-octahydrobenzo[b]pyrano[3,2-f][1,5]oxazocin-8-yl)-4-(trifluoromethyl)benzamide (30 mg, 65 umol, 1.0 equiv) and triethylamine (45.1 uL, 0.32 mmol, 5.0 equiv) in CH₂Cl₂ (1.2 mL). After 15 min, the iced bath was removed and the reaction mixture was stirred at rt overnight. Silica gel was then added and the crude was concentrated to dryness. Purification was done via silica gel chromatography (gradient: 5–65% EtOAc in Hexanes) affording isobutyl (((2S,4aS,12aR)-5-methyl-6-oxo-8-(4-(trifluoromethyl)benzamido)-2,3,4,4a,5,6,12,12a-octahydro-

benzo[b]pyrano[3,2-f][1,5]oxazocin-2-yl)methyl)carbamate (16.6 mg, 29 umol, 46 % yield) as a white powder. Alternatively, the title compound was also prepared from N-((2S,4aS,12aR)-2-(aminomethyl)-5-methyl-6-oxo-2,3,4,4a,5,6,12,12a-octahydrobenzo[b]pyrano[3,2-f][1,5]oxazocin-8-yl)-4-(trifluoromethyl)benzamide and isobutylchloroformate (1.1 equiv), in a mixture of 1,4-dioxane and saturated aqueous sodium bicarbonate solution (dioxane:sat. NaHCO₃=2:1, 0.05M concentration), at 0 °C. Upon completion of the reaction (LCMS, 2h), extraction of the mixture with EtOAc followed by evaporation of the solvents afforded a crude residue which was purified on silica using the same conditions as described above. ¹H NMR (400 MHz, CDCl₃) δ 9.69 (br s, 1H), 8.04 (br d, J = 8.0 Hz, 1H), 7.99 (d, J = 8.1 Hz, 2H), 7.67 (d, J = 7.9 Hz, 2H), 7.47 (s, 1H), 6.74 (d, J = 9.0 Hz, 1H), 5.08 – 4.99 (m, 1H), 3.93 (d, J = 14.7 Hz, 1H), 3.90 – 3.79 (m, 2H), 3.79 – 3.66 (m, 2H), 3.59 (br s, 1H), 3.55 – 3.40 (m, 2H), 3.19 (s, 3H), 3.12 – 3.00 (m, 1H), 2.15 – 2.00 (m, 2H), 1.93 (ddd, J = 13.7, 6.9, 6.9 Hz, 1H), 1.86 – 1.74 (m, 1H), 1.63 (br d, J = 13.7 Hz, 1H), 0.95 (s, 3H), 0.93 (s, 3H). ¹³C NMR (100 MHz, CDCl₃) δ 170.8, 165.1, 157.1, 150.9, 138.9, 133.0 (q, JC-F = 32.9 Hz), 132.3, 128.3, 125.4 (q, JC-F = 3.6 Hz), 124.8, 123.9 (q, JC-F = 272.6 Hz), 123.4, 119.8, 119.3, 77.8, 71.4, 64.9, 51.0, 45.6, 32.2, 28.2, 24.5, 23.6, 19.1. LRMS (ESI) calcd for C₂₈H₃₃F₃N₃O₆ [M + H]⁺ 564.23, found 564.13.

Characterization of 4:

(S)-N-(((2S,4aS,12aR)-5-methyl-6-oxo-8-(4-(trifluoromethyl)benzamido)-2,3,4,4a,5,6,12,12a-octahydrobenzo[b]pyrano[3,2-f][1,5]oxazocin-2-yl)methyl)tetrahydrofuran-2-carboxamide:

¹H NMR (400 MHz, CDCl₃) δ 9.69 (s, 1H), 8.06 (d, J = 8.7 Hz, 1H), 8.00 (d, J = 7.8 Hz, 2H), 7.68 (d, J = 7.9 Hz, 2H), 7.49 (s, 1H), 7.04 (br s, 1H), 6.73 (d, J = 9.0 Hz, 1H), 4.36 (dd, J = 7.0 Hz, 1H), 4.01 – 3.83 (m, 3H), 3.79 – 3.66 (m, 2H), 3.65 – 3.42 (m, 3H), 3.23 (s, 4H), 2.37 – 2.24 (m, 1H), 2.15 – 1.99 (m, 3H), 1.99 – 1.71 (m, 3H), 1.68 – 1.57 (m, 1H). LRMS (ESI) calcd for C₂₈H₃₁F₃N₃O₆ [M + H]⁺ 562.22, found 562.44.

Characterization of 5:

N-((2S,4aS,12aR)-2-(((5-cyclobutyl-1,3,4-oxadiazol-2-yl)amino)methyl)-5-methyl-6-oxo-2,3,4,4a,5,6,12,12a-octahydrobenzo[b]pyrano[3,2-f][1,5]oxazocin-8-yl)-4-(trifluoromethyl)benzamide: ¹H NMR (400 MHz, CDCl₃) δ 9.01 (s, 1H), 8.01 (d, J = 7.8 Hz, 2H), 7.93 (br d, J = 9.0 Hz, 1H), 7.72 (d, J = 8.0 Hz, 2H), 7.49 (s, 1H), 6.80 (d, J = 9.0 Hz, 1H), 5.97 (br s, 1H), 4.14 – 4.00 (m, 1H), 3.88 – 3.72 (m, 4H), 3.70 – 3.54 (m, 1H), 3.37 – 3.25 (m, 1H), 3.23 (s, 3H), 2.47 – 2.33 (m, 4H), 2.22 – 2.06 (m, 3H), 2.06 – 1.95 (m, 1H), 1.94 – 1.79 (m, 1H), 1.78 – 1.67 (m, 1H). LRMS (ESI) calcd for C₂₉H₃₁F₃N₅O₅ [M + H]⁺ 586.23, found 586.25.

Conclusions

Current report presents a DOS-derived molecule with remarkable effects on lipid metabolism in hepatic cells. BRD8518, initially identified as an inducer of expression of the

cardioprotective gene *TRIB1*, turned out to broadly reprogram the lipoprotein metabolism in HepG2 cells from lipogenesis driven VLDL secretion to lipid scavenging through LDL uptake. This activity profile is unique as currently used cardiovascular drugs lower the blood lipid levels either by stimulating LDL clearance through elevation of hepatic LDL uptake (statins by inducing LDL receptor expression or PCSK9 blocking antibodies by reducing the LDL receptor degradation) or by reducing hepatic production of VLDL particles, the precursor to LDL particles (e.g. MTTP inhibitor lomitapide or ApoB targeting anti-sense oligonucleotide mipomersen). BRD8518 appears to regulate both arms of lipoprotein metabolism and to combine both activities in one molecule. The limiting ADME properties of BRD8518 were remedied by medicinal chemistry efforts that led to identification of cpd **3**, which has enhanced potency and improved pharmacokinetic properties. Development of cpd **3**, a new lead in the series of tricyclic glycol class of *TRIB1* inducers, should enable future *in vivo* proof of concept studies and will facilitate target identification efforts.

Conflicts of interest

There are no conflicts to declare.

Acknowledgements

This work was sponsored in part by the Broad Institute Gift and the National Institutes of Health (NIH) Molecular Libraries Probe Production Centers Network (MLPCN) Program. The authors wish to thank Amy Deik for conducting LC-MS analyses, Melissa Bennion, Chaewon Hwang and Katie Loveluck for expert technical assistance.

References

1. Teslovich TM, Musunuru K, Smith AV, Edmondson AC, Stylianou IM, Koseki M, et al. Biological, clinical and population relevance of 95 loci for blood lipids. *Nature*. 2010;466(7307):707-13.
2. Ishizuka Y, Nakayama K, Ogawa A, Makishima S, Boonvisut S, Hirao A, et al. *TRIB1* downregulates hepatic lipogenesis and glycogenesis via multiple molecular interactions. *Journal of molecular endocrinology*. 2014;52(2):145-58.
3. Consortium CAD, Deloukas P, Kanoni S, Willenborg C, Farrall M, Assimes TL, et al. Large-scale association analysis identifies new risk loci for coronary artery disease. *Nat Genet*. 2013;45(1):25-33.
4. Musunuru K, Romaine SP, Lettre G, Wilson JG, Volcik KA, Tsai MY, et al. Multi-ethnic analysis of lipid-associated loci: the NHLBI CARE project. *PLoS One*. 2012;7(5):e36473.
5. Walia GK, Gupta V, Aggarwal A, Asghar M, Dudbridge F, Timpson N, et al. Association of common genetic variants with lipid traits in the Indian population. *PLoS One*. 2014;9(7):e101688.
6. Aung LH, Yin RX, Wu DF, Li Q, Yan TT, Wang YM, et al. Association of the *TRIB1* tribbles homolog 1 gene rs17321515 A>G polymorphism and serum lipid levels in the Mulao and Han populations. *Lipids Health Dis*. 2011;10:230.
7. Burkhardt R, Toh SA, Lagor WR, Birkeland A, Levin M, Li X, et al. *Trib1* is a lipid- and myocardial infarction-associated gene that regulates hepatic lipogenesis and VLDL production in mice. *J Clin Invest*. 2010;120(12):4410-4.
8. Satoh T, Kidoya H, Naito H, Yamamoto M, Takemura N, Nakagawa K, et al. Critical role of *Trib1* in differentiation of tissue-resident M2-like macrophages. *Nature*. 2013;495(7442):524-8.
9. Schreiber SL. Organic chemistry: Molecular diversity by design. *Nature*. 2009;457(7226):153-4.
10. Gerard B, Lee MDt, Dandapani S, Duvall JR, Fitzgerald ME, Kesavan S, et al. Synthesis of stereochemically and skeletally diverse fused ring systems from functionalized C-glycosides. *The Journal of organic chemistry*. 2013;78(11):5160-71.
11. Nagiec MM, Skepner AP, Negri J, Eichhorn M, Kuperwasser N, Comer E, et al. Modulators of hepatic lipoprotein metabolism identified in a search for small-molecule inducers of tribbles pseudokinase 1 expression. *PLoS One*. 2015;10(3):e0120295.
12. Akella LB, Marcaurelle LA. Application of a sparse matrix design strategy to the synthesis of dos libraries. *ACS Comb Sci*. 2011;13(4):357-64.
13. Mulrooney CA, Lahr DL, Quintin MJ, Youngsaye W, Moccia D, Asiedu JK, et al. An informatic pipeline for managing high-throughput screening experiments and analyzing data from stereochemically diverse libraries. *J Comput Aided Mol Des*. 2013;27(5):455-68.
14. Peck D, Crawford ED, Ross KN, Stegmaier K, Golub TR, Lamb J. A method for high-throughput gene expression signature analysis. *Genome biology*. 2006;7(7):R61.
15. Tullai JW, Schaffer ME, Mullenbrock S, Sholder G, Kasif S, Cooper GM. Immediate-early and delayed primary response genes are distinct in function and genomic architecture. *J Biol Chem*. 2007;282(33):23981-95.
16. Cao A, Wu M, Li H, Liu J. Janus kinase activation by cytokine oncostatin M decreases PCSK9 expression in liver cells. *J Lipid Res*. 2011;52(3):518-30.
17. Pak YK, Kanuck MP, Berrios D, Briggs MR, Cooper AD, Ellsworth JL. Activation of LDL receptor gene expression in HepG2 cells by hepatocyte growth factor. *J Lipid Res*. 1996;37(5):985-98.
18. Do HT, Tselykh TV, Makela J, Ho TH, Olkkonen VM, Bornhauser BC, et al. Fibroblast growth factor-21 (FGF21) regulates low-density lipoprotein receptor (LDLR) levels in cells via the E3-ubiquitin ligase Mylip/Idol and the Canopy2 (Cnpy2)/Mylip-interacting saposin-like protein (Msap). *J Biol Chem*. 2012;287(16):12602-11.
19. Yashiro T, Nanmoku M, Shimizu M, Inoue J, Sato R. 5-Aminoimidazole-4-carboxamide ribonucleoside stabilizes low density lipoprotein receptor mRNA in hepatocytes via ERK-dependent HuR binding to an AU-rich element. *Atherosclerosis*. 2013;226(1):95-101.
20. Vargas NB, Brewer BY, Rogers TB, Wilson GM. Protein kinase C activation stabilizes LDL receptor mRNA via the JNK pathway in HepG2 cells. *J Lipid Res*. 2009;50(3):386-97.
21. Schmittgen TD, Livak KJ. Analyzing real-time PCR data by the comparative C(T) method. *Nature protocols*. 2008;3(6):1101-8.
22. Carvalho BS, Irizarry RA. A framework for oligonucleotide microarray preprocessing. *Bioinformatics*. 2010;26(19):2363-7.
23. K. SG. Limma: linear models for microarray data. *Bioinformatics and computational biology solutions using R and Bioconductor*: Springer New York; 2005. p. 397-420.

